Performance Analysis of Alternative Refrigents Inside Capillary Tube of Refrigeration System

B.N.C. Mohan Reddy [1], J.A.Sandeepkumar [2], A.V. Hari Babu[3]

1. Department of Mechanical Engineering, SVR College of Engineering, Nandyal-518501, INDIA

2. Department of Mechanical Engineering, SVR College of Engineering, Nandyal-518501, INDIA

3. Department of Mechanical Engineering, SVR College of Engineering, Nandyal-518501, INDIA

Abstract

The chlorofluorocarbon (CFCs) and hydro-chlorofluorocarbon (HCFCs) refrigerants are being replaced by hydro-fluorocarbons (HFCs) due to environmental concerns about depletion of the earth's protective stratospheric ozone layer and global climate change. A refrigeration system using new alternative refrigerants must be modified or newly designed because the thermo-physical properties of these alternative refrigerants differ from those of conventional refrigerants. In order to maintain or improve the performance of the cycle, the operating characteristics of individual components of the system should be clarified for use with the new alternative refrigerants.

. In this work, a full array of methane and ethane derivatives were considered and the trade-off in flammability, toxicity and chemical stability concerning atmospheric lifetime with changes in molecular chlorine, fluorine and hydrogen content were carried out. Therefore, two single-fluid alternative refrigerants (R410a and R134a) that contain no chlorine were selected for the investigation along with R22.In the present investigation, the performance of alternative refrigerants in an adiabatic capillary tube was investigated using ANSYS CFX in a vapour compression refrigeration system. The proposed model predicts the flow characteristics in adiabatic capillary tube for a given mass flow rate. In the present study alternative refrigerants R-22, R-134a and R-410a are used as working fluids inside a straight capillary tube of diameter 1.27mm and used the same model to study the flow characteristics of refrigerants. The mass flow rate is compared for these refrigerants and best suited refrigerant is suggested.

The mass flow rates of R-134a and R410a were 34.828% higher and 2.22% lower than that of R-22 respectively. As a result R-410a is a good substitute for R-22 but only the compressor size should be increased as the pressures are 50% higher than that of R-22.

Keywords- *Refrigerants- R22- R-134a - R410-AANSYS CFX–massflow rates- shapes.*

I. INTODUCTION

The chlorofluorocarbon (CFCs) and hydro-chlorofluorocarbon (HCFCs) refrigerants are being replaced by hydro-fluorocarbons (HFCs) due to environmental concerns about depletion of the earth's protective stratospheric ozone layer and global climate change. A refrigeration system using new alternative refrigerants must be modified or newly designed because the thermo-physical properties of these alternative refrigerants differ from those of conventional refrigerants. In order to maintain or improve the performance of the cycle, the operating characteristics of individual components of the system should be clarified for use with the new alternative refrigerants.

Capillary tubes, short tube orifices and thermostatic expansion valves have been used in refrigerators and heat pumps as refrigerant flow regulating devices in vapour compression plants for several years. Capillary tubes and short tube orifices are constant area expansion devices. In some cases, they can substitute more expensive and complex thermostatic valve. The principle of operation of the capillary tube is the flow resistance caused by a long, narrow tube, throttling the refrigerant pressure. Pressure falls gradually as the liquid flows through the tube, until it starts to evaporate in the tube. This vapour formation, called "vapour lock", causes a sudden pressure drop in approximately the last quarter of the length, down to the evaporator pressure. The capillary tube is a simple drawn copper tube with an inner diameter ranging from 0.5 to 2.0 mm and a length ranging from 400 to 2500 mm. The flow inside the capillary tube is complex because of phase change and pressure drop through the capillary tube has a strong influence on the performance of the whole system

II. LITERATURE REVIEW

Capillary tube is very small in the recent years the work on separated flow model considering slip between the liquid and vapour phases have started picking up. A part from this the theoretical as well as experimental work is usually divided into two groups that is adiabatic capillary tubes and Non Adiabatic capillary tubes.

Akure et al. [1] has discussed the effects of various geometries of capillary tubes had been investigated by many researchers. Their studies were based on the coil diameters and lengths alone, no particular attention had been placed on the effect of coil pitch. At present no information is available about the effects of serpentine-coiled capillary tubes on refrigerator performance. This study examined the effects of pitches of both helical and serpentine-coiled capillary tubes on the performance of a vapour compression refrigeration system. Several capillary tubes of equal lengths (2.03 m) and varying pitches, coiled diameters and serpentine heights were used. Both inlet and outlet pressure and temperature of the test section (capillary tube) were measured and used to estimate the coefficient of performance (COP) of the system. The results show that, in the case of helical-coiled geometries the pitch has no significant effect on the system performance but the coil diameter as already predicted by many researchers. In the case of serpentine geometries both pitch and height affects the system performance. Performance increases with both increase in the pitch and the height. Correlations were proposed to describe relationships between straight and coiled capillary tube and between helical-coiled and serpentine-coiled capillary tubes. The coefficient of correlations are: 0.9841 for mass flow rates of helical and serpentine with straight tubes; 0.9864 for corresponding COPs and 0.9996 for mass flow rates of serpentine and helical-coiled tube.Bansal and Rupasinghe [2] has also developed an empirical model for sizing capillary tubes. This paper presents an empirical model that has been developed to size adiabatic and non-adiabatic capillary tubes for small vapour compression refrigeration systems, in particular,household refrigerators and freezers. The model is based on the assumption that the length of a capillary tube is dependent on five primary variables, namely the capillary tube inner diameter, the mass flow rate of the refrigerant in the capillary tube, the pressure difference between high side and low side, the refrigerant sub cooling at capillary inlet and the relative roughness of the capillary tube material. The model is validated with previous studies over a range of operating conditions and is found to agree reasonably well with the experimental data for HFCI34a.

Bansal and Rupasinghe [3] have presented a homogeneous two-phase flow model, CAPIL, which is designed to study the performance of adiabatic capillary tubes in small vapour compression refrigeration systems, in particular household refrigerators and freezers. The model is based on the fundamental equations of conservation of mass, energy and momentum that are solved simultaneously through iterative procedure and Simpson's rule. The model uses empirical correlations for single-phase and two-phase friction factors and also accounts for the entrance effects. The model includes the effect of various design parameters, namely the tube diameter, tube relative roughness, tube length, level of sub cooling and the refrigerant flow rate. The model is validated with earlier models over a range of operating conditions and is found to agree reasonably well with the available experimental data for HFC-134a.

Bansal and Wang [4] proposed a homogeneous simulation model for choked flow conditions for pure refrigerants (R134a, R600a) in adiabatic capillary tubes. The model is based on the first principles of thermodynamics and fluid mechanics and some empirical relations. This study presents a fresh-look at the classical fluid flow problem, known as Fanno flow for refrigerant flow in capillary tubes. A new diagram called the full range simulation diagram has been developed that presents a better way to understand the choked flow phenomenon graphically. The diagram is useful for design and analysis of refrigerant flow in capillary tubes. The model has been validated with published experimental data for R22, R134a and R600a and is found to agree to within ±7%.

A mathematical model has been developed to predict the performance of a helical capillary tube under adiabatic flow conditions has also been developed by Khan et al. [5]. The proposed model can predict the length of the adiabatic helical capillary tube for a given mass flow rate or the mass flow rate through a given length of capillary tube. The effect of parameters like condensing pressure, degree of sub cooling, pitch of helix and the coil diameter has been studied for the flow of refrigerant R-134a through the adiabatic helical capillary tube. A capillary tube selection chart has been developed, using the proposed model, to predict the mass flow rate of refrigerant R-134a through a capillary of size 1.07 mm diameter and 2 m length.

Khan et al. [6] have also developed a numerical model flow through an adiabatic spiral capillary tube. An analytical model has been developed to predict the length of adiabatic capillary tubes used in domestic refrigerators and low-capacity residential air

conditioners. The model predicts the length of two types of tubes—straight and spiral adiabatic capillary tubes. The proposed model is based on the homogenous two-phase flow model, which predicts the length of the adiabatic capillary tubes as a function of refrigerant mass flow rate, capillary tube diameter, degree of sub cooling at capillary inlet, internal surface roughness, and the pitch of the Archimedean spiral. The existence of sub cooled liquid at the entry of the capillary tube requires the computation of single-phase and then two-phase lengths of the tube. McAdams et al. [7] viscosity correlation has been used to evaluate the two-phase viscosity of the expanding refrigerant in the latter part of the capillary tube. The simulation results are validated with the experimental findings of previous researchers. The performance of the above two geometries of adiabatic capillary tube is compared, and it is established that for the same state of refrigerants at the inlet and exit of the adiabatic capillary, spiral capillary is found to have a shorter length. Parametric study of the adiabatic capillary tubes is also carried out. Further, the effect of geometric and physical parameters has been presented in detail. A much smaller capillary tube is required when the eco-friendly refrigerants R-134a and R-152a are used in place of refrigerant R-12 for similar conditions across the adiabaticspiral capillary tube.

Khan et al. [8] have presented a comprehensive review of the literature on the flow of various refrigerants through the capillary tubes of different geometries viz. straight and coiled and flow configurations viz. adiabatic and diabatic. The literature has been presented in chronological order the experimental and numerical investigations systematically under different categories. Flow aspects like effect of coiling and effect of oil in the refrigerants on the mass flow rate through the capillary tube have been discussed. The paper also provides key information about the range of input parameters viz. tube diameter, tube length, surface roughness, coil pitch and coil diameter, inlet sub cooling and condensing pressure or temperature. Other information includes type of refrigerants used, correlations proposed and methodology adopted in the analysis of flow through the capillary tubes of different geometries operating under adiabatic and diabatic flow conditions. It has been found from the review of the literature that there is a lot more to investigate for the flow of various refrigerants through different capillary tube geometries.

In the literature Sami et al [9], explained the experimental data obtained on capillary tube behaviour, using various new alternatives under different geometrical parameters will be presented and analysed. Capillary geometrical parameters will include length, diameter, as well as entrance conditions. The results clearly showed that the pressure drop across the capillary tube is significantly influenced by the diameter of the capillary tube, inlet conditions to the capillary and refrigerant type. The data demonstrated that the capillary pressure drop decreases with the increase of the capillary diameter and that alternatives in general experience higher pressure drop than that of R-.

Wongwises and Pirompak [10] have studied the flow characteristics of pure refrigerants and refrigerant mixtures in adiabatic capillary tubes and this paper provides the results of simulations using an adiabatic capillary tube as a refrigerant control device in refrigerating systems. The developed model can be considered as an effective tool of capillary tubes' design and optimization for systems using newer alternative refrigerants.

III. THEORY OF CAPILLARY TUBE

Capillary tubes have been investigated in detail for many decades. A capillary tube is a common expansion devices used in small sized refrigeration and air-conditioning systems. A capillary tube is a constant area expansion device used in vapour-compression refrigeration systems located between the condenser and the evaporator and whose function is to reduce the high pressure in the condenser to low pressure in the evaporator. The capillary tube expansion devices are widely used in refrigeration equipment especially in small units such as household refrigerators, freezers and small air conditioners. Its simplicity is the most important reason to continue using it instead of other expansion devices. Capillaries substitute for more expensive and complex thermostatic valves. For instance, capillary tubes are used in some complex cooling systems for particle detectors installed. Nevertheless, one can find other reasons for their use in highly specialized cooling circuits.

In fact the flow through capillary tube is actually adiabatic not an isenthalpic. As the name suggests the adiabatic capillary tubes are one in which there is no heat transfer with the surroundings or the walls of capillary tube are thermally insulated. On the basis of geometrical shape the capillary tubes are classified under:

- Straight capillary tube
- Coiled capillary tube

A. *Straight Capillary Tube*

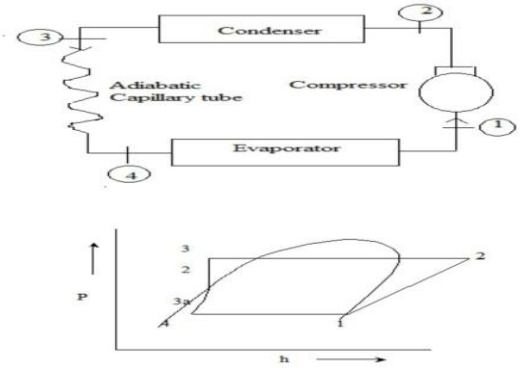

Figure 3.1 Adiabatic Capillary tube (a) block diagram (b) p-h diagram

Figure 3.1a shows the vapour compression system employing the adiabatic capillary tube as an expansion device. The process 3-4 in figure 3.1b represents adiabatic expansion of the high pressure liquid refrigerant. The refrigerant temperature remains constant as long as it is in liquid state and as the flashing of refrigerant occurs (at point 3a) the pressure as well as temperature falls rapidly. As the flow through the capillary tube is adiabatic, the enthalpy is refrigerant remains constant till the flashing occurs. As a result of flashing, a part of enthalpy is used to increase the kinetic energy of the refrigerant. Therefore, as the vaporization progresses the enthalpy of refrigerant falls ion the two-phase flow region of the capillary tube , as can be seen from the Figure 3.1b.

In adiabatic capillary tube, the refrigerant expands from higher pressure side to lower pressure side with no heat exchange with the surroundings. The refrigerant often enters the capillary in a sub cooled liquid state. As the liquid refrigerant flows through the capillary, the pressure drops linearly due to friction while the temperature remains constant. As the pressure of refrigerant falls below the saturation pressure a fraction of liquid refrigerant flashes into vapour. The fluid velocity increases because of the fall in density of the refrigerant due to vaporization. Thus, the entire capillary tube length seems to be divided into two distinct regions. The region near entry is occupied by the liquid phase and the other as the two-phase liquid vapour region.

The flow inside the capillary tube of refrigeration system can be divided into a sub cooled liquid region from the entrance to the point in which the fluid reaches saturated conditions and a two-phase flow region after that point until the end of the capillary tube. In figure 3.2, the variation of refrigerant temperature and pressure has been plotted against the capillary tube length. The pressure falls linearly in the liquid region of the capillary tube while the temperature remains constant as the flow through capillary tube is adiabatic. Further, as the pressure falls below the saturation pressure, Ps with the onset of vaporization both temperature and pressure starts falling rapidly until the choked flow conditions are attained.

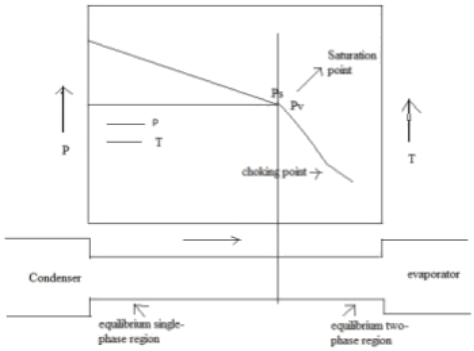

Figure 3.2 Temperature and Pressure variation along adiabatic capillary tube

However, in reality ,after the flow reaches the saturation pressure, there is a short region in which the evaporation does not start and the refrigerant becomes superheated, Chen et al., Chang and Ro. The liquid in this region is not in thermodynamic equilibrium but under metastable condition. This region end up quite suddenly and the liquid starts to evaporate approaching thermodynamic two-phase equilibrium conditions.

B. *Coiled Capillary Tubes*

The helical capillary tube in a domestic refrigerator or in a window air conditioner are no more a new thing. The difference between the consecutive turns of the coiled capillary tube is termed as coil pitch denoted by ‘p’. In helical capillary tube there are two coiling parameters one is coil pitch and another is coil diameter. Figure 3.3 shows helical and spiral tubes depicting the geometric parameters, viz. coil pitch, coil diameter and tube diameter.

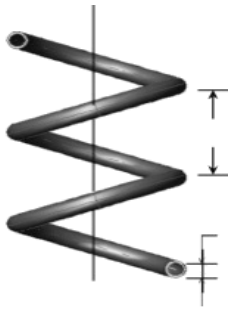

Figure 3.3 Helically Coiled Capillary tubes

The flow through coiled tube is complicated comparing to straight tubes. The frictional pressure drop of a single phased fluid flow through a curved tube is larger than that for a flow through a straight tube under similar conditions. The fluid flowing in tube undergoes a centrifugal force, which results in secondary flow, as shown in figure 3.3. The secondary flow imposed on the main flow forms a counter-rotating helical vortex pair. The existence of secondary flow is called the Dean effect. Dean has proposed a dimensionless number called Dean number given by the following equation.

$$De = Re\sqrt{} \quad \ldots\ldots\ldots\ldots\ldots\ldots\ldots (3.1)$$

The flow pattern by Dean's analysis is shown in figure 3.4. The secondary flow in the coiled tube has the stabilizing effect on laminar fluid flow, resulting in higher critical Reynolds number increases with the increase in ratio, d/D, and is expressed by the following relation proposed by Ito [4].

$$Re_{crit}=\frac{d}{D}\ldots\ldots\ldots\ldots\ldots\ldots\ldots\ldots\ldots\ldots (3.2)$$

C. Vapour-compression cycle:

The vapour-compression cycle is used in most household refrigerators as well as in many large commercial and industrial refrigeration systems. In this cycle, a circulating refrigerant such as Freon enters the compressor as a vapour. From point1 and point2, the vapour is compressed at constant entropy and exists the compressor as a vapour at a higher temperature, but still below the vapour pressure at that temperature, from point2 and point3 and on to the point 4, the vapour travels through the condenser which cools the vapour until it starts condensing, and then condenses the vapour into liquid by removing additional heat at constant pressure and temperature. Between points 4 and 5, the liquid refrigerant goes through the expansion valve (also called as throttle valve) where its pressure abruptly decreases, causing flash evaporation and auto-refrigeration of, typically, less than half of the liquid.

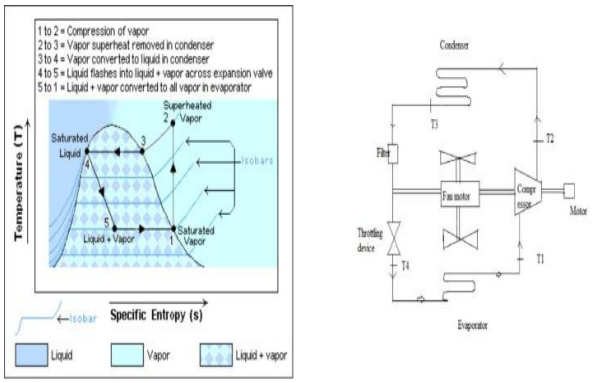

Figure 3.5 Vapour Compression cycle

That results in mixture of liquid and vapour at a lower temperature and pressure as shown at point 5. The cold liquid-vapour mixture then travels through the evaporator coil or tubes and is completely vaporized by cooling the warm air (from the space being refrigerated) being blown by a fan across the evaporator coil or tubes. The resulting refrigerant vapour returns to the compressor inlet at point 1 to complete the thermodynamic cycle.

IV. EXPERIMENTAL SETUP

A. Details of Experimental setup of air conditioning:

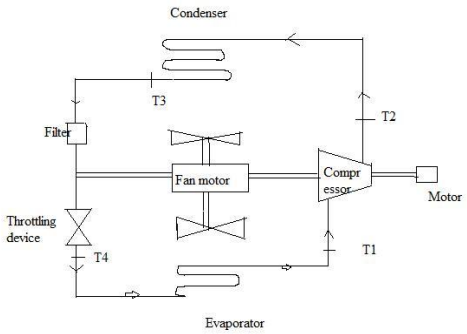

Figure 4.1 Schematic diagram of Air-conditioning system

As shown in the figure 4.1 schematic diagram of Air-conditioning system is shown. The main components of the system is compressor, condenser, throttling device, evaporator etc.

B. Specifications of the system :

Compressor: 1 TR (hermitically sealed)
Condenser: Air cooled
Evaporator: Air cooled
Throttling Device: Capillary tube straight
Refrigerant: R- ($CHCLF_2$)
Control Panel: 220 AC
Voltmeter Reading (V), Ammeter Reading (A)
Main switch with 6 channel temperature indicator
T_1- Inlet temperature of compressor
T_2- Outlet temperature of compressor
T_3- Outlet of condenser
T_4- Temperature after throttling
T_5- Air temperature at blower outlet
T_6- Ambient temperature
Knobs: For filling refrigerant.

1. Throttling device : straight capillary tube of diameter 1.27 mm and length 762 mm
2. Viewer : liquid line indicator viewer after condenser before throttling

C. Compressor operating pressure range :

Inlet pressure: 65-90 (Psi), Outlet pressure: 225-310 (Psi)

Switches thermostat controller 1 -2 C

1. Compressor + fan (low speed)
2. Compressor + fan (high speed)
3. Compressor + fan (medium speed)

D. Experimental Results :

The experiment is conducted on air-conditioning system with a straight capillary tube the following values are obtained.

Table 4.1 Temperature readings

T_1	T_2	T_3	T_4	T_5	T_6
32^{O}C	3˚C	52˚C	5˚C	3 ˚C	39˚C

Hence the capillary tube inlet temperature is T_{in} =52 C
And capillary tube outlet temperature is T_{out} = 11.5 C
Corresponding pressures are P_{in} = 13.628 bar and P_{out} = 6.686 bar
Mass flow rate m = 40.73 kg/h

V. COMPUTATIONAL MODELLING

A. Computational Fluid Dynamics

Due to the fast development of computer power during the past decade, the usage of CFD has increased enormously. The purpose with CFD is to analyse systems involving fluid dynamics, heat transfer and other associated phenomena such as chemical reactions and phase changes by numerical calculations. The areas of application are very large and cover both industrial and none industrial territories. Some examples of these follow:

- Flow and heat transfer in industrial processes (boilers, heat exchangers, combustion equipment, pumps, blowers, piping, etc.).
- Aerodynamics of ground vehicles, aircrafts, missiles.
- Film coating, thermoforming in material processing applications.
- Flow and heat transfer in propulsion and power generation systems.
- Ventilation, heating and cooling flows in buildings.
- Chemical Vapour Decomposition (CVD) for integrated circuit manufacturing.
- Heat transfer for electronics packaging applications.
- Sports, Biomedical, Chemical.
- Materials Processing, Micro fluids.

B. The Structure of CFD

CFD codes are all structured around the numerical algorithms that will solve the fluid flow problems. The CFD code consists of the following three fundamental features:

1. Pre-processor
2. Solver
3. Post-processor

1. Pre-Processor:

Pre-processor consists of the input of a flow problem to a CFD program by means of an operator-friendly interface and the subsequent transformation of this input into a form suitable for use by the solver. Pre-processing stage involves:

- Fixing the domain
- Generation of Grids
- Selection of physical and chemical phenomena
- Definition of fluid properties and
- Specification of appropriate boundary conditions

2. Solver:

The solver uses information from the pre-processing stage to approximate unknown flow variables by means of functions, discretize governing flow equations and solving the equations. The numerical methods that form the basis of solver perform the following steps:

- Approximation of the unknown flow variables by means of simple function
- Discretisation by substitution of the approximation into the governing flow equations and subsequent mathematical manipulations
- Solution of the algebraic equations
- The main differences between the three separate streams are associated with the way in which the flow variables are approximated and with the discretization process.

3. Post-Processor:

Post-Processing is the process to examine and analyse the flow field problems. Post-Processor includes anything which is as follows:

- Animation of fluid flow
- Contours plots

- Vector plots
- Animation of stream lines
- Numerical Calculations
- Iso-surfaces and CFD Uncertainty Analysis
-

C. Overview of the solution methodology in ANSYS-CFX

ANSYS-CFX is an integrated software system capable of solving diverse and complex multi-dimensional fluid flow problems. The fluid solver provides solutions for incompressible or compressible, steady-state or transient, laminar or turbulent single phase fluid flow in complex geometries. The software uses block-structured non-orthogonal grids with grid embedding and grid attaching to discretize the domain. Discretization of the governing equations is achieved by discretizing the domain into finite control volumes using a mesh. The governing equations are integrated over each control volume in such a way that mass; momentum, energy etc. are conserved in a discrete sense for each control volume.

D. Governing Equations

The fluid properties associated with fluid flow problems include those that can be identified for a fluid at rest, and those transport properties identified for a flowing fluid. In order to solve any fluid flow problem, information is required on the properties of the fluid. All fluids have specific properties which define their state or condition and which describe their behaviour under various processes. Thermodynamic properties are those properties which are related to assigning the energy of a fluid and include temperature, pressure, density and enthalpy. Once thermodynamic properties are known, there is sufficient detail to describe the fluid as it remains at rest.

However, fluid flow problems, generally deal with fluids which are in motion. In this case, transport properties are necessary to define the dynamic processes occurring in the fluid. Examples of transport properties of the viscosity, thermal conductivity and diffusion coefficient. The expressions vand explanations of the relationship between properties used in ANSYS-CFX are presented.

E. Equation of state:

For an ideal gas, the equation of state is defined as

Pv = RT

where R is universal gas constant divided by the molecular weight of the fluid.

F. Equation of state for enthalpy:

For real gases, the enthalpy may be considered to consist of two components: a perfect gas component (C_pT) and correction.

$$h = h_{ref} + \int_{T_1}^{T_2} c_p(T, P_1)\, dT + \int_{P_1}^{P_2} \left[V - T_2\left(\frac{\partial V}{\partial T}\right)_p\right] dP$$

Integration is performed along a line of constant P in first step, and then along a line of constant T in second step.

G. Mass conservation equation:

$$\frac{\partial \rho}{\partial t} + \frac{\partial}{\partial x_j}(\rho U_j) = 0$$

In this equation U_j represents the three dimensional velocity vector components of the flow. If the flow is assumed steady, then

$$\boldsymbol{\frac{\partial U_j}{\partial x_j} = 0}$$

H. Momentum conservation equation:

The conservation equation for momentum, ρU_i , can be formulated as

$$\frac{\partial}{\partial_t}(\rho U_i) + \frac{\partial}{\partial x_i}(\rho U_i U_j) = -\frac{\partial P}{\partial x_i} - \frac{\partial \tau_{ij}}{\partial x_j} + \partial f_i$$

The three terms on right hand side of above equation represent the x components of all force due to the pressure P, the viscous stress tensor τ_{ij} , and the body force f_i. For a Newtonian fluid, the stress tensor is given by

$$\boldsymbol{\tau_{ij} = -\mu_b \delta_{ij}\left(\frac{\partial U_i}{\partial x_i} + \frac{\partial U_j}{\partial U_j} + \frac{\partial U_k}{\partial U_k}\right) - \mu\left(\frac{\partial U_i}{\partial U_j} + \frac{\partial U_j}{\partial U_i}\right)}$$

Where $\mu_b = 2/3\mu$ is bulk viscosity and δ_{ij} represents the Kronecker delta ($\delta_{ij} = 1$ fr i=j and $\delta_{ij} = 0$ for $i \neq j$).

For flows in rotating frames of reference, the effects of the Coriolis and centripetal forces are modeled in the code. In this case

$$\vec{f_i} = -\left(2\vec{\Omega} \times \vec{U} + \vec{\Omega} \times (\vec{\Omega} \times \vec{r})\right)$$

where vector notation has been used Ω is the rotation velocity and r is the location vector.

I. Energy conservation equation:

Besides mass and momentum, energy is third fluid property for which a conservation equation in terms of the total enthalpy, H is given by

$$\frac{\partial}{\partial t}(\rho H) + \frac{\partial}{\partial x_j}\left(\rho U_j H\right) = \frac{\partial Q_j}{\partial x_j} + \rho U_i f_i$$

where H = h + 1/2 U_iU_i , h = static enthalpy.
If dissipation is small, neglecting pressure and dissipation terms

$$\frac{\partial}{\partial t}(\rho H) + \frac{\partial}{\partial x_j}\left(\rho U_j H\right) = \frac{\partial Q_j}{\partial x_j} + \rho U_i f_i$$

In a rotating frame of reference, the rothalpy, I, is advected in place of the total enthalpy, H. The equation for I is given by
$I = H - \omega^2 R^2 / 2$
where ω the rotation rate and R is in the local radius.

J. Turbulence Models:

Turbulence models modify the original unsteady Navier-Stokes equations by the introduction of averaged fluctuating components to produce the RANS equations. Turbulence models based upon RANS equations are known as statistical turbulence models due to the statistical averaging procedure adopted for obtaining the equations. Though the process greatly enhances the speed of computation, the averaging process results in additional unknown terms containing the products of unknown quantities. These are referred to as turbulent/Reynolds stresses. These Reynolds stresses are to be modelled in order to obtain the closure and various equations used to describe this determine the turbulence model.

K. Reynolds- Averaging:

For any arbitrary quantity U the decomposition into mean and fluctuating part can be written as

$U=\bar{U} + u$

$$\bar{U} = \lim_{\Delta t \to x}\left(\frac{1}{\Delta t}\right)\int_{t}^{t+\Delta t} U dt$$

Where Δt is the time scale selected in such a way that it is larger in comparison to trubulent fluctuations, but smaller in comparison to the time scale to which the equations are solved. Substituting the time averaged quantities in the original transport equations:

$$\frac{\partial \rho}{\partial t} + \frac{\partial}{\partial x_j}\left(\rho \overrightarrow{U_J}\right) = 0$$

$$\frac{\partial}{\partial t}\left(\rho \overrightarrow{U_i}\right) + \frac{\partial}{\partial x_j}\left(\rho \overrightarrow{U_i U_j}\right) = -\frac{\partial \bar{P}}{\partial x_i} - \frac{\partial}{\partial x_j}\left(\overline{\tau_{ij}} + \rho \overline{u_i u_j}\right) + \rho f_i$$

$$\frac{\partial}{\partial t}(\rho \bar{H}) + \frac{\partial}{\partial x_j}(\rho \overline{U_i H}) = -\frac{\partial}{\partial x_j}\left(\overline{Q_j} + \rho \overline{u_j H}\right) + \rho \overline{U_i} f_i$$

$$\bar{H} = \bar{h} + \frac{1}{2}\overline{U_i}\overline{U_j} + k$$

where k represents the turbulent kinetic energy for an incompressible flow.

L. The standard k-ε turbulence model

The **k-ε**turbulence model utilizes the eddy-viscosity assumption to relate the Reynolds stress and turbulent flux terms to the mean flow variables.

M. Continuity equation

$$\frac{\partial p}{\partial t} + \frac{\partial}{\partial x_j}\left(\rho \overline{U_j}\right) = 0$$

Momentum equation

$$\frac{\partial}{\partial t}\left(\rho \overline{U_i}\right) + \frac{\partial}{\partial x_j}\left(\rho \overline{U_i U_j}\right) = -\frac{\partial P}{\partial x_i} + \frac{\partial}{\partial x_j}\left\{\mu_{eff}\left[\frac{\partial \overline{U_i}}{\partial x_j} + \frac{\partial \overline{U_j}}{\partial x_j}\right] - \frac{2}{3}\mu_{eff}\left(\frac{\partial \overline{U_i}}{\partial x_i} + \frac{\partial \overline{U_j}}{\partial x_j} + \frac{\partial \overline{U_k}}{\partial x_k}\right)\right\}$$

$\mu_{eff}=\mu+\mu_t$
μ_t=turbulent viscosity
and$P^*=P+2/3\rho K$
Turbulent viscosity is related to turbulent kinetic energy k and dissipation rate ε as

$$\mu_t = \rho\, c_\mu \frac{k^2}{\varepsilon}$$

The values of k and ε come directly from the differential transport equations for turbulent kinetic energy and turbulent dissipation rate as:

$$\frac{\partial(\rho k)}{\partial t} + \frac{\partial\left(\rho \overline{U_j} k\right)}{\partial x_j} = \frac{\partial}{\partial x_j}\left[\Gamma_k \frac{\partial k}{\partial x_j}\right] + p_k - \rho\varepsilon$$

$$\frac{\partial(\rho\varepsilon)}{\partial t} + \frac{\partial\left(\rho \overline{U_j}\varepsilon\right)}{\partial x_j} = \frac{\partial}{\partial x_j}\left[\Gamma_k \frac{\partial \varepsilon}{\partial x_j}\right] + \frac{\varepsilon}{k}\left(c_{\varepsilon 1} p_k + \rho c_{\varepsilon 2}\varepsilon\right)$$

where diffusion coefficients are given by

$$\Gamma_k = \mu + \frac{\mu_t}{\sigma_k}$$

$$\Gamma_\varepsilon = \mu + \frac{\mu_t}{\sigma_\varepsilon}$$

whereσ_k and σ_ε are model constants.

Production rate of turbulent kinetic energy $p_k$is given by

$$p_k = \{\mu_t \left[\frac{\partial \bar{U}_i}{\partial x_j} + \frac{\partial \bar{U}_j}{\partial x_i}\right]\frac{\partial \bar{U}_i}{\partial x_j} - \frac{2}{3}[\rho k + \mu_t\left(\frac{\partial \bar{U}_i}{\partial x_i} + \frac{\partial \bar{U}_j}{\partial x_j} + \frac{\partial \bar{U}_k}{\partial x_k}\right)]\}\frac{\partial U_k}{\partial U_k}$$

The values of constants in the model are $c_\mu = 0.09$,$c_{\varepsilon 1}$= 1.44, $c_{\varepsilon 2}$= 1.92, σ_k=1.0 , σ_ε=1.3 and Turbulent prandtl number Pr_t=0.9

N. Finite volume formulation

ANSYS-CFX uses a finite-element-based finite volume method. The governing equations namely the conservation for mass: momentum and energy are expressed as

$$\frac{\partial \rho}{\partial t} + \frac{\partial}{\partial X_j}(\rho \bar{U_j}) = 0$$

$$\frac{\partial}{\partial t}(\rho u_i) + \frac{\partial}{\partial t}(\rho u_i u_j) = -\frac{\partial P}{\partial x_i} + \frac{\partial}{\partial x_j}\left\{\mu_{eff}\left[\frac{\partial u_i}{\partial x_j} + \frac{\partial u_j}{\partial x_i}\right]\right\} + S_{ui}$$

$$\boldsymbol{\frac{\partial}{\partial t}(\rho \emptyset) + \frac{\partial}{\partial t}(\rho u_j \emptyset) = \frac{\partial}{\partial x_j}\{\Gamma_{eff}\left[\frac{\partial \emptyset}{\partial x_j}\right]\} + S_\emptyset}$$

where the energy conservation has been replaced by a generic scalar transport equation. The finite volume method proceeds by integrating these equations over a fixed control volume, which, suing Gauss Theorem, results in,

$$\frac{\partial}{\partial t}\int \rho dV + \int_\varepsilon \rho u_j dn_j = 0$$

$$\frac{\partial}{\partial t}\int_v \rho u_{idV} + \int_\varepsilon \rho u_j u_i dn_j = -\int_\varepsilon P dn_j + \int_\varepsilon \mu_{eff}\left(\frac{\delta u_i}{\delta x_j}\right)dn_j + \int_v S_{u_i} dV$$

$$\frac{\partial}{\partial t}\int_v \rho \emptyset dv + \int_\varepsilon \rho u_j \emptyset dn_j = \int_\varepsilon \Gamma_{eff}\left(\frac{\delta \emptyset}{\delta X_j}\right)dn_j + \int_v S \emptyset dv$$

where v and s denote volume and surface integrals respectively and dn_j represents the differential Cartesian component of the outward normal surface vector.

The equations represent a flux balance in a control volume. The above equations are applied to each control volume or cell in the computational domain. These continuous equations are approximated numerically using discrete functions. Discretization of the above equations yields the following:

$$\rho V\left(\frac{\rho - \rho^\circ}{\Delta t}\right) + \sum_{i[}(\rho u_j \Delta n_j)_{ip} = 0$$

$$\rho V\left(\frac{u_i - u_i^\circ}{\Delta t}\right) + \sum_{ip} m_{ip}(u_i)_{ip} = \sum_{ip}(P\Delta n_i)_{ip} + \sum_{ip}\left(\mu_{eff}\left(\frac{\partial u_i}{\partial X_j} + \frac{\partial u_j}{\partial X_i}\right)\Delta n_j\right)_{ip} + \overline{S_u}V$$

$$\rho V\left(\frac{u_i - u_i^\circ}{\Delta t}\right)\sum_{ip} m_{ip}\emptyset_{ip} = \sum_{ip}\left(\Gamma_{eff}\frac{\partial \emptyset}{\partial X_j}\Delta n_j\right)\overline{S_u}V$$

where

$$\boldsymbol{M_{ip} = (\rho u_j \Delta n_j)_{ip}^0}$$

and V is volume of the control volume, the subscript ip denotes the integration point, the summation is over all the integration points of the surface, Δn_j is the discrete outward surface vector, Δt is the time step, the superscript o refers to the old time level, and the over bar on the source terms indicate an average value for the control volume. The fluxes are evaluated at integration points, which are shared by adjacent control volumes and exactly the same flux that leaves one control volume enters the next.

The discretization in ANSYS-CFX is of four types. First one is upwind difference the conventional upwind difference scheme. Second one is mass weighted scheme, which is more accurate than upwind difference scheme and slightly less robust than upwind difference scheme. Third one is modified linear profile, which is modified to reduce negative coefficients in high transverse flow Peclet number situations, and is very accurate and gives second order error reduction in most instances, but is less robust. Fourth one is linear profile skew, which is more accurate and truly second order, but is the least robust.

O. Boundary conditions

Boundary conditions are specified for each boundary face. Each boundary control volume equation is ultimately closed when each boundary condition specification for each boundary face has been implemented. In general, boundary conditions can affect the control volume closure in any one of the two ways:

P. Flux Discretised Boundary Conditions

The flow of the conserved quantity throughеach of the four boundary integration point surfaces is evaluated using the information provided by the boundary condition specification and control volume values within the element local to the face. These flow estimates are inserted into each of the four boundary control volumes sharing the boundary face. Boundary conditions implemented in this way include: Walls, inlets, outlets and symmetry planes.

Q. Domain Transformation Boundary Conditions:

The boundary control volume istransformed or combined with other boundary control volumes, in a manner consistent with the boundary condition specification such that the flow through the boundary surface vanishes. Usually domain transformation boundary conditions bring together two or more boundary control volumes to affect the desired boundary condition. Boundary conditions implemented in this way include periodic boundary conditions, grid embedding interfaces, grid attaching interfaces, and many-to-one periodic connections.

VI. PROBLEM STATEMENT

Capillary tubes are widely used as a refrigerant flow control device in small refrigeration systems. Since the flow behaviour inside the capillary tube is complex because of phase change, many physical models are necessary to predict the characteristics of the refrigerant flow in a capillary tube. Two phase flow through adiabatic capillary tube is analysed with alternative refrigerants R22, R134a and R410a. Due to environmental concerns about depletion of earth's protective stratospheric ozone layer and global climate change the chlorofluorocarbon and hydro-chlorofluorocarbon refrigerants are replaced by hydro-fluorocarbons. So to find out the best refrigerant which has zero ozone depletion potential and lower global warming potential three alternative refrigerants are taken and the flow characteristics are analysed and best suited refrigerant is suggested.

A) Straight Capillary Tube:

Straight Capillary tube is modelled in ANSYS Workbench. The diameter of the tube is 1.27mm and length of the tube is 762mm.

1) Model:

The model of the straight capillary tube is shown in the figure:

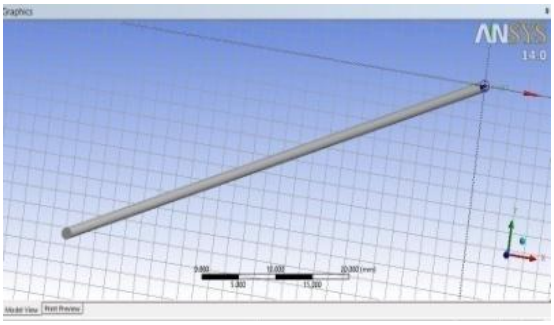

Figure 6.1 Model of the Straight Capillary tube

2) Mesh:

Meshing of a model is very important in ansys. Proper meshing of the model gives better results, and it reduces the iteration time for solving.The following diagram gives information about meshing procedure of the model. Inflation mesh is taken outer surface of the tube.

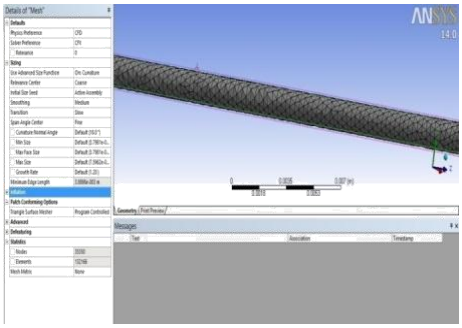

Figure 6.2 Straight Capillary tube meshing

B. Grid Independence Study

To test grid independence the pressure at the capillary tube exit was measured at different grid resolutions and is presented in the table below. All calculations are done with mesh number 2 with 35,350 nodes.

Table 6.1 Grid Independence Study

S. No.	Nodes	Outlet Static Pressure in Pascal's
1	33,364	1.870e+06
2	35,350	1.905e+06
3	35,873	1.937e+06

C. Boundary Conditions

After creation of CFX mesh, In ANSYS CFX module the materials are imported from material library. A list of refrigerant R22vl is suitable requires two-phase flow analysis. These boundary conditions are summarized and tabulated below. The domain of the fluid is R-22. The inlet boundary conditions and outlet boundary conditions are taken from the experimental values. The inlet boundary condition is taken as normal speed 8.4 m/s and static temperature 52˚C. The outlet boundary conditions is taken as static pressure 6.686 bar and heat transfer is taken as adiabatic. Similarly the boundary conditions for R-134a and R-410a are tabulated in table 6.3 and table 6.4.

Table 6.2 Boundary Details for straight Capillary tube when R-22 is taken as refrigerant

Domain	Fluid	R-22
	Fluid 1	R-22l
	Fluid 2	R-22v
	Heat Transfer	Thermal Energy
	Turbulence	k-Epsilon
	R22l	Equilibrium
	R22v	Equilibrium
Boundary inlet	Flow regime	Subsonic
	Normal speed	8.4m/s
	Turbulence	Medium (intensity =
	Static Temperature	52˚C
Boundary Outlet	Flow regime	Subsonic
	Static Pressure	6.686 bar
Boundary Wall	Wall Roughness	Smooth wall
	Heat Transfer	Adiabatic

Domain	Fluid	R-134a
	Fluid 1	R-134al
	Fluid 2	R-134av
	Heat Transfer	Thermal Energy
	Turbulence	k-Epsilon
	R134al	Equilibrium Constraint
	R134av	Equilibrium Fraction
Boundary Outlet	Flow regime	Subsonic
	Normal Speed	5 m/s
	Turbulence	Low (intensity = 1%)
	Static Temperature	32˚C
Boundary Wall	Flow regime	Subsonic
	Static Pressure	3 bar
	Wall Roughness	Smooth Wall
	Heat Transfer	Adiabatic

Domain	Fluid	R-134a
	Fluid 1	R-134al
	Fluid 2	R-134av
	Heat Transfer	Thermal Energy
	Turbulence	k-Epsilon
	R134al	Equilibrium Constraint
	R134av	Equilibrium Fraction
Boundary inlet	Flow regime	Subsonic
	Normal Speed	5 m/s
	Turbulence	Low (intensity = 1%)
	Static Temperature	32˚C
	Flow regime	Subsonic
	Static Pressure	3 bar

Boundary Outlet	Wall Roughness	Smooth Wall
	Heat Transfer	Adiabatic

After the select of default domain default tab and select the wall as ANSYS CFX creates the wall adiabatic by default and the model acting as a working fluid. By solving the model with solver and the results are obtained through CFX-Post.

VII. RESULTS AND DISCUSSIONS

In this chapter, the results obtained from the experimental model R22 are compared with the commercially available software ANSYS CFX module and the effect of flow properties on the refrigerants R-22, R-134a and R-410a inside straight capillary tube are studied. The mass flow rates for all these refrigerants are compared and best refrigerant is suggested.

A. Validation of computational Results of R22

The results obtained by computational model of straight capillary tube with refrigerant R22 by using ansyscfx is validated with experimental results of R22. Once the results are validate with experimental results, then mass flow rates for refrigerants R22, R134a and R410a are compared.

1) Experimental results of straight capillary tube with R22 as refrigerant

Experiment is conducted on air-conditioning system, straight capillary tube readings are obtained. The inlet temperature of the capillary tube is 52˚C and outlet temperature of the capillary tube is 11.5˚C. The corresponding pressures at inlet 13.628 bar and at outlet 6.686 bar. At inlet of the capillary tube mass fraction of the R-22 liquid is 1 and mass fraction of R-22 vapour is 0. At outlet of the capillary tube mass fraction of the R-22 liquid is 0.7205 and mass fraction of R-22 vapour is 0.2795.

2) Computational results of straight capillary tube with R-22 as refrigerant

For the study of flow properties inside the straight capillary tube R-22, R-134a and R-410a are used as working fluids. Further study the effect of fluid properties such as pressure, temperature, mass fraction of liquid and vapour on length.

3) Comparison of Computational results of R-22 with experimental results of R-22

After the completion of both experimental and computational, the results obtained are tabulated below. The results are shown in table 7.1. The computational results obtained are approximately same with respect to experimental values.

Table 7.1 Properties of Experimental and Computational for straight capillary tube with R-22 as refrigerant

Properties	Experimental	Computational
Inlet Temperature(Tin)	52˚C	51.9˚C
Outlet Temperature(Tout)	11.5˚C	13.4˚C
Inlet Pressure(Pin)	13.628 bar	12.68 bar
Outlet Pressure(Pout)	6.686 bar	6.406 bar
Inlet mass fraction of R-22l	1	1
Outlet mass fraction of R-22l	0.7205	0.7537
Inlet mass fraction of R-22v	0	0
Outlet mass fraction of R-22v	0.2795	0.2463

From the table 7.1 the results of both experimental and computational are approximate. Hence the computational results are validated with experimental results for refrigerant R-22.

B. When R-22 is used as refrigerant in the straight capillary tube

When R-22 is used as refrigerant inside the capillary tube the following flow properties vary and the variations of pressure, temperature, mass fraction of liquid and vapour are shown.

*1) **Pressure variation***

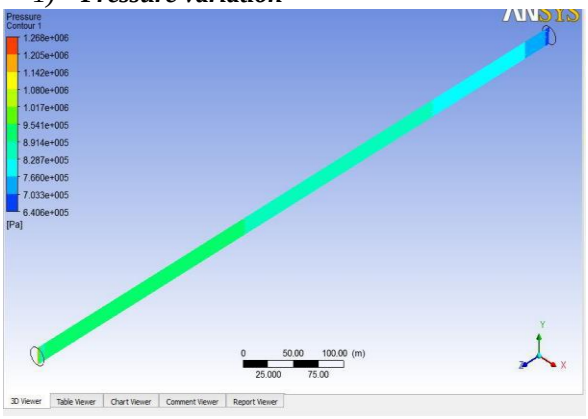

Figure 7.1 Pressure in straight capillary tube

Figure 7.1 has been drawn to compare the computational pressures with experimental results, to study the flow characteristics for R-22 inside the straight capillary tube. The results obtained from the existing model predict the pressures as to ANSYS CFX. As the refrigerant enters the capillary tube its pressure drops linearly. As refrigerant enters in the two-phase region there is a sharp decrease in pressure and temperature this is due to cumulative effect of friction drop and acceleration pressure drop, which leads to more vaporization of the fluid into two-phase region. The pressure contours are shown in figure 7.1. The main function of the capillary tube is to decrease the pressure of the capillary tube so the pressure is decreased from 12.68 bar to 6.406 bar and from the experimental calculations, the pressures are from 13.628 bar to be decreased to 6.686 bar which is fair to be in agreement.

*2) **Temperature variation***

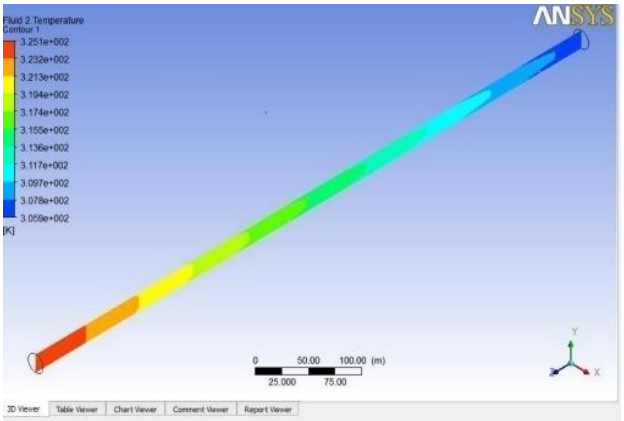

Figure 7.2 Temperature in the straight capillary tube

The temperature contours are shown in figure 7.2. The main function of capillary tube is to decrease the temperature of the capillary tube so the temperature decrease is observed from 52˚C to 11.5˚C and from the experimental calculations, the temperatures are from 51.9˚C to be decreased to 13.4˚C which is fair to be in agreement.

*3) **Mass Fraction Contour of liquid and vapour***

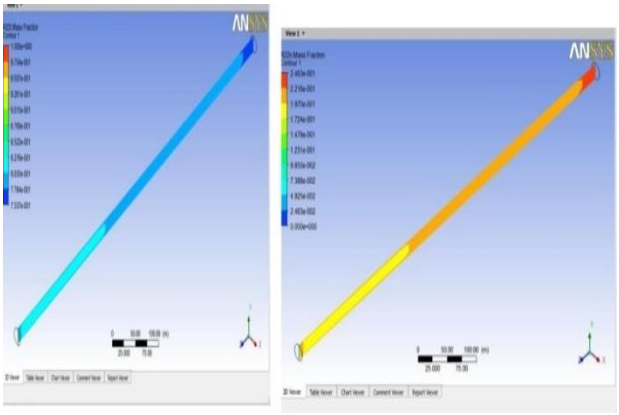

Figure 7.3 (a) liquid mass fraction in straight capillary tube
(b) vapour mass fraction in straight capillary tube

The liquid mass fraction contours are shown in figure 7.3 (a). The main function of the capillary tube is to decrease the mass fraction of the capillary tube so the mass fraction of liquid decrease is observed 1 to 0.753 and the experimental calculations are measured to be from 1 to 0.7205 which is fair to be in agreement.

The vapour mass fraction contours are shown in the figure 7.3 (b). The main function of the capillary tube is to increase in mass fraction of vapour of the capillary tube so the mass fraction of vapour is observed from 0 to 0.2463 and the experimental calculations are measured to be from 0 to 0.2795 increase is observed which is fair to be in agreement.

D) Graphs

The fluid properties of R-22 along the length are plotted below

7.2.4.1 Pressure and temperature graphs of straight capillary tube

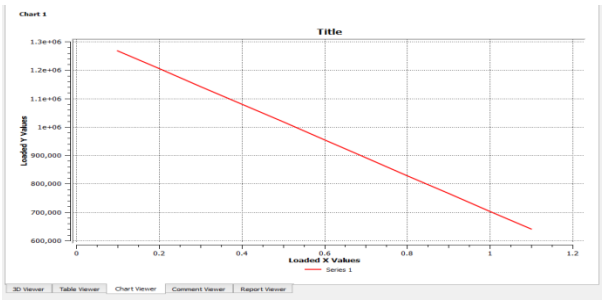

(a)

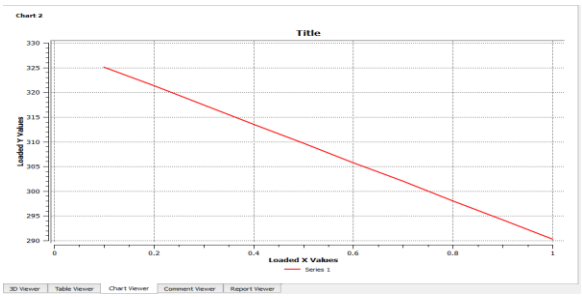

(b)

Figure 7.4 (a) Pressure graph of straight capillary tube along the length
(b) Temperature graph of straight capillary tube along the length

As shown in figure 7.4 (a) and (b) the pressure and temperature decreases linearly up to certain length from inlet to outlet. The flow reaches before the exit point the pressure and temperature decreases drastically.

7.2.4.2 Vapour mass fraction graph of straight capillary tube

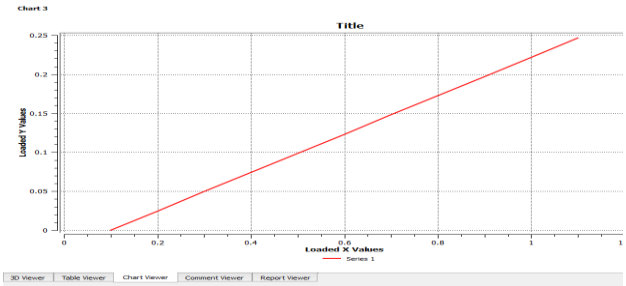

Figure 7.5 Vapour mass fraction graph of R-22 in straight capillary tube

From the graphs figure 7.5, mass fraction of vapour is increasing from inlet to outlet along the length of the capillary tube hence mass fraction of liquid decreases from inlet to outlet.

C. *When R-134a is used as refrigerant in straight capillary tube*

When R-134a is passed into the straight capillary tube the following flow properties vary and the flow variations of pressure, temperature, mass fraction of liquid and vapour are shown below.

7.3.1 Pressure Variation

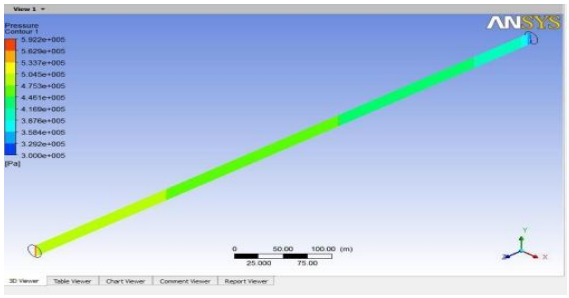

Figure 7.6 Pressure of R-134a in straight capillary tube

Figure 7.6 has been drawn to study the flow characteristics for R-134a inside the straight capillary tube. The results obtained from the existing model predicts the pressures from ANSYS CFX.
The pressure contours are shown in the figure 7.6. The main function of the capillary tube is to decrease the pressure of the capillary tube so the pressure is decreased from 5.922 bar to 3 bar.

7.3.2 Temperature Variation

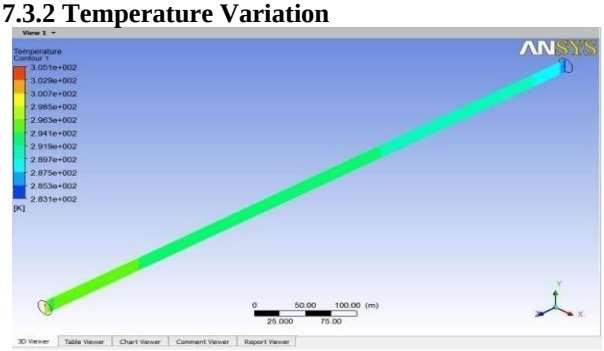

Figure 7.7 Temperature variation of R-134a in straight capillary tube

The temperature contours are shown in the figure 7.7. The main function of the capillary tube is to decrease the temperature of the capillary tube so the temperature decrease is observed from 32˚C to 10.1˚C.

7.3.3 Mass fraction of liquid and vapour

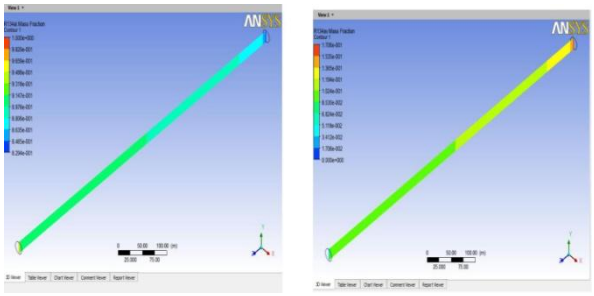

Figure 7.8 (a) liquid mass fraction of R-134a in straight capillary tube
(b) vapour mass fraction of R-134a in straight capillary tube

The liquid mass fraction contours are shown in figure 7.8 (a). The main function of the capillary tube is to decrease the mass fraction of the capillary tube so the mass fraction of liquid decrease is observed from 1 to 0.8294.

The vapour mass fraction contours are shown in figure 7.8 (b). The main function of the capillary tube is to increase the mass fraction of vapour of the capillary tube so the mass fraction of vapour increase is observed from 0 to 0.1706.

7.3.4 Graphs

7.3.4.1 Pressure and Temperature graphs of R-134a in straight capillary tube

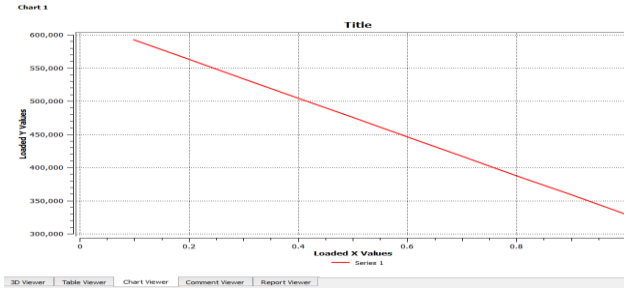

(a)

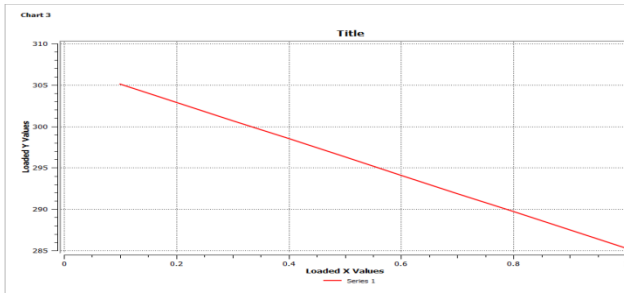

(b)

Figure 7.9 (a) Pressure graph of R-134a inside straight capillary tube along length

(b) Temperature graph of R-134a inside straight capillary tube along length

As shown in the figure 7.9 (a) and (b) the pressure and temperature decreases along the length of the capillary tube linearly up to certain length from inlet to outlet . The flow reaches before the exit point the pressure and temperature decreases drastically.

7.3.4.2 Vapour mass fraction graph of straight capillary tube

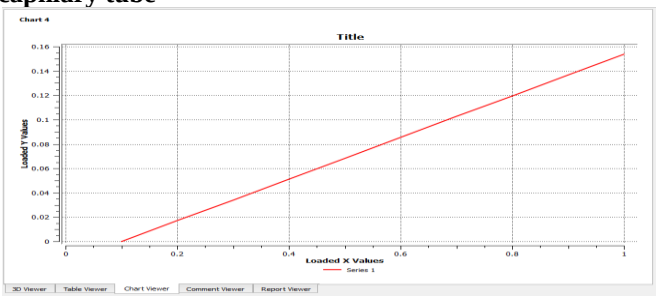

Figure 7.10 Vapour mass fraction graph of R-134a inside straight capillary tube

From the graphs figure 7.10, mass fraction of vapour is increasing from inlet to outlet hence mass fraction of liquid decreases from inlet to outlet.

7.2 Computational Comparison of mass flow rates of R-22, R-134a and R-410a

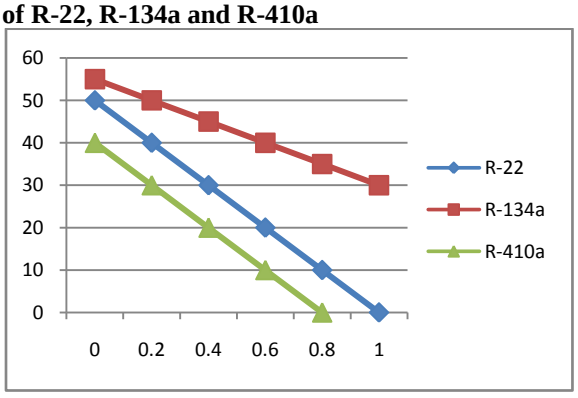

Figure 7.11 Effect of capillary tube length on mass flow rate of refrigerants

As shown in the figure, the mass flow rate is approximately inversely proportional to length of the capillary tube length. An increase in the length of the capillary tube length will increase the friction loss in the tube, which will reduce the mass flow rate of the refrigerant. In this figure there is no much difference between mass flow rates of R-22 and R-410a. The average mass flow rate of R-134a and R-410a are 34.828% higher and 2.22% lower than R-22 respectively.

VIII. CONCLUSIONS AND FUTURE SCOPE

A. *Conclusions*

Two phase flow through capillary tube is analysed with three alternative refrigerants R22, R134a and R410a. The flow through capillary tube is complex because of phase change from liquid to vapour. Experiment is conducted on adiabatic capillary tube for obtaining boundary conditions. A two-phase CFD model is developed and experimental results are validated and simulation models for alternative refrigerants R134a and R410a for straight capillary are developed using ANSYS CFX module. The mass flow rates of all these refrigerants are compared and best suited refrigerant for refrigeration system is suggested. The following conclusions are drawn

- The experimental model is setup and the experimental values of straight capillary tube with R-22 as refrigerant are taken, and the computational results are validated.
- In addition to R-22, two other alternative refrigerants R-134a and R-410a are analysed and flow characteristics of these two refrigerants are studied.
- The mass flow rate of R-134a was 34.828% higher than that of R-22.
- The mass flow rate of R-410a was 2.22% lower than that of R-22.
- The mass fraction of vapour for R410a is 45% which is very much higher than that of R-22. As maximum amount of liquid is turning into vapour R-410a gives best performance.
- As a result R-410a is a good substitute for R-22 but only the compressor size should be increased as the pressures are 50% higher than that of R-22.
- It is suggested that R-410a gives best performance since it has Zero Ozone Depletion and very near characteristics of R-22.

REFERENCES

[1] Akure, Ondo State, Nigeria, " Effect of Coiled Capillary Tube Pitch on VapourCompression Refrigeration System Performance", AU J.T. 11(1), p 14-22, Jul. 2007.

[2] Bansal PK, Rupasinghe AS. 1996. An empirical model for sizing capillary tubes. International Journal of Refrigeration Vol. 19: 497-505.

[3] Bansal PK, Rupasinghe AS. 1998. A homogenous model for adiabatic capillary tubes. Applied Thermal Engineering Vol. 18: 207-219.

[4] Bansal, P.K. and Wang, G., Numerical analysis of choked refrigerant flow in adiabatic capillary tubes Applied Thermal Engineering, Vol. 25, pp. 2014-2028, 2003.

[5] Khan, M. K., Kumar, R., Sahoo, P.K., 2008. Experimental and Numerical Investigations of the Flow of R-134a Through Lateral Type Diabatic Capillary Tube, HVAC&R Research ASHRAE, Vol. 14, issue 6, pp. xxx-xxx. (in press).

[6] Khan, M.K., Kumar, R., Sahoo, P.K., Flow Characteristics of Refrigerants Flowing through Capillary Tubes - A Review, Applied Thermal Engineering, (available online on http://sciencedirect.com) 2007.

[7] McAdams, W.H., Wood, W.K. and Bryan, R.L, Vaporization inside Horizontal Tubes-Part II: Benzene-Oil Mixture, Trans. ASME, Vol. 64, p. 193, 1942.

[8] Khan, M.K., Kumar, R., Sahoo, P.K., 2008. A Homogenous Flow Model for Adiabatic Helical Capillary Tube, ASHRAE Transactions, Vol. 114, Part 1, pp. 239-249.

[9] Sami, S. M., Maltais, H. and Desjardins, D. E.,Influence of Geometrical Parameters on Capillary Behaviour with New Alternative Refrigerants, MechanicalEngineering, School of Engineering University of Moncton, Moncton, NB, E1A 3E9.

[10] Wongwises S, Pirompak W. 2001. Flow characteristics of pure refrigerants and refrigerant mixtures in adiabatic capillary tubes. Applied Thermal Engineering Vol. 21: 845-861.